Journal Pre-proofs

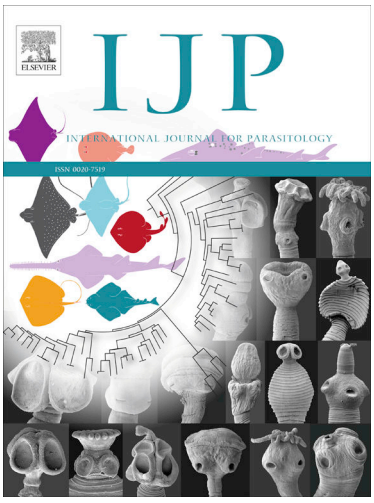

Identification and characterization of sirtuin enzymes in cestodes and evaluation of sirtuin inhibitors as new cestocidal molecules

Hugo Rolando Vaca, Ana María Celentano, María Agustina Toscanini, Alexander-Thomas Hauser, Natalia Macchiaroli, María Luján Cuestas, Alejandro David Nusblat, Wolfgang Sippl, María Celina Elissondo, Manfred Jung, Federico Camicia, Mara Cecilia Rosenzvit

PII: S0020-7519(22)00015-7
DOI: https://doi.org/10.1016/j.ijpara.2021.12.002
Reference: PARA 4464

To appear in: *International Journal for Parasitology*

Received Date: 15 October 2021
Revised Date: 14 December 2021
Accepted Date: 14 December 2021

Please cite this article as: Vaca, H.R., Celentano, A.M., Toscanini, M.A., Hauser, A-T., Macchiaroli, N., Cuestas, M.L., Nusblat, A.D., Sippl, W., Elissondo, M.C., Jung, M., Camicia, F., Rosenzvit, M.C., Identification and characterization of sirtuin enzymes in cestodes and evaluation of sirtuin inhibitors as new cestocidal molecules, *International Journal for Parasitology* (2022), doi: https://doi.org/10.1016/j.ijpara.2021.12.002

Identification and characterization of sirtuin enzymes in cestodes and evaluation of sirtuin inhibitors as new cestocidal molecules

Hugo Rolando Vaca[a,b], Ana María Celentano[a,b,1], María Agustina Toscanini[a,b,c,1], Alexander-Thomas Hauser[d], Natalia Macchiaroli[e], María Luján Cuestas[a,b], Alejandro David Nusblat[c], Wolfgang Sippl[f], María Celina Elissondo[g,h], Manfred Jung[d], Federico Camicia[i,*], Mara Cecilia Rosenzvit[a,b,*]

[a]*Departamento de Microbiología, Parasitología e Inmunología, Facultad de Medicina, Universidad de Buenos Aires (UBA), Ciudad Autónoma de Buenos Aires, Argentina.*

[b]*Universidad de Buenos Aires (UBA). CONICET. Instituto de Investigaciones en Microbiología y Parasitología Médica (IMPaM), Ciudad Autónoma de Buenos Aires, Argentina.*

[c]*Universidad de Buenos Aires (UBA). CONICET. Instituto de Nanobiotecnología (NANOBIOTEC), Ciudad Autónoma de Buenos Aires, Argentina.*

[d]*Institute of Pharmaceutical Sciences, University of Freiburg, Freiburg, Germany.*

[e]*Laboratorio de Genómica y Bioinformática de Patógenos, Instituto de Biociencias, Biotecnología y Biología Traslacional (iB3), Departamento de Fisiología y Biología Molecular y Celular, Facultad de Ciencias Exactas y Naturales, Universidad de Buenos Aires (UBA), Buenos Aires, Argentina.*

[f]*Institute of Pharmacy, Martin-Luther-University of Halle-Wittenberg, Halle(Saale), Germany.*

[g]*Instituto de Investigaciones en Producción Sanidad y Ambiente (IIPROSAM CONICET-UNMdP); Facultad de Ciencias Exactas y Naturales – UNMdP; Centro Científico Tecnológico Mar del Plata – CONICET; Centro de Asociación Simple CIC PBA, Mar del Plata, Argentina.*

[h]*Laboratorio de Zoonosis Parasitarias, Facultad de Ciencias Exactas y Naturales, Universidad Nacional de Mar del Plata, Mar del Plata, Argentina.*

[i]*Laboratorio de Toxinopatología, Centro de Patología Experimental y Aplicada, Facultad de Medicina, Universidad de Buenos Aires (UBA), Ciudad Autónoma de Buenos Aires, Argentina.*

[1]These authors contributed equally to this work.

*Corresponding authors. *E-mail addresses*: fcamicia@fmed.uba.ar (Federico Camicia); mrosenzvit@fmed.uba.ar (Mara Cecilia Rosenzvit)

Note: Supplementary data associated with this article.

Abstract

Anti-parasitic treatment of neglected tropical diseases (NTDs) caused by cestodes such as echinococcosis and cysticercosis relies on a small number of approved anthelmintic drugs. Furthermore, the treatment is usually prolonged and often partially effective and not well tolerated by some patients. Therefore, the identification of novel drug targets and their associated compounds is critical. In this study, we identified and characterized sirtuin (SIRT) enzymes in cestodes and evaluated the cestocidal potential of SIRT inhibitors. SIRTs are a highly conserved family of nicotinamide-adenine dinucleotide (NAD^+)-lysine deacylases involved in multiple cellular functions. Here, we described the full repertoire of SIRT-encoding genes in several cestode species. We identified six SIRT-encoding genes that were classified into SIRTs Class I (SIRT1, SIRT2, and SIRT3), Class III (SIRT5), and Class IV (SIRT6 and SIRT7). In *Echinococcus* spp., SIRT genes showed transcriptional expression throughout several developmental stages, SIRT2 being the most expressed. To evaluate the potential of SIRT inhibitors as new cestocidal molecules, we determined the in vitro effect of several Class I SIRT inhibitors by motility assay. Of those, the selective SIRT2 inhibitor Mz25 showed a strong cestocidal activity in *Mesocestoides vogae* (syn. *Mesocestoides corti*) tetrathyridia at various concentrations. The Mz25 cestocidal activity was time- and dose-dependent with a half-maximal inhibitory concentration (IC_{50}) value significantly lower than that of albendazole. Additionally, Mz25 induced extensive damage in the general morphology with marked alterations in the tegument and ultrastructural features. By homology modeling, we found that cestode SIRT2s showed a high conservation of the canonical SIRT structure as well as in the residues related to Mz25 binding. Interestingly, some non-conservative mutations were found on the selectivity pocket (an Mz25-induced structural rearrangement on the active site), which represent a promising lead for developing selective cestode SIRT2 inhibitors derived from Mz25. Nevertheless, the Mz25 molecular target in *M. vogae* is unknown and remains

to be determined. This report provides the basis for further studies of SIRTs to understand their roles in cestode biology and to develop selective SIRT inhibitors to treat these parasitic NTDs.

Keywords: Cestodes, Neglected tropical diseases, *Echinococcus*, *Mesocestoides vogae*, Sirtuins, Mz25

1. Introduction

Sirtuin (SIRT) enzymes are a unique class of lysine deacylases highly conserved in all kingdoms of life, ranging from bacteria to humans. These enzymes were initially classified as Class III histone deacetylases (HDACs). However, SIRTs require nicotinamide-adenine dinucleotide (NAD^+) as a catalytic cofactor, which differs from HDACs that use a zinc only-catalyzed mechanism, and show no sequence homology to the zinc-dependent enzymes. Due to their unique NAD^+-dependent mechanism, the catalytic activity of SIRTs is not restricted to acetyl groups, being also able to remove other acyl groups (such as myristoyl, palmitoyl, crotonyl, glutaryl, and succinyl) from the ε-amino group of lysines in histones and other non-histone proteins (Schiedel et al., 2018). These properties make SIRTs a very special class within the lysine deacylase superfamily. As a result of this multitude of protein substrates, SIRTs are involved in key cellular processes including transcription, metabolic sensing, inflammation, and apoptosis (Finkel et al., 2009; Schiedel et al., 2018). Thus, SIRTs represent promising targets for pharmaceutical intervention. In humans, seven SIRT-encoding genes (SIRT1-7) have been identified and classified into four classes: Class I (SIRT1, SIRT2, and SIRT3), Class II (SIRT4), Class III (SIRT5), and Class IV (SIRT6 and SIRT7) (Frye, 2000). In parasites, several SIRT-encoding genes were identified and evaluated as drug targets in *Plasmodium falciparum*, *Schistosoma mansoni*, *Leishmania* spp., and *Trypanosoma cruzi* (Fioravanti et al., 2020).

Cestodes, also known as tapeworms, are an important group of parasites (class Cestoda) in the phylum Platyhelminthes. Several cestode species cause diseases such as echinococcosis and cysticercosis which represent a significant problem in human and animal health. Both echinococcosis and cysticercosis are recognized by the World Health Organization as neglected tropical diseases (NTDs) (World Health Organization, 2020). These diseases disproportionately affect socioeconomically vulnerable populations, representing serious public health problems in

many developing countries around the world (Budke et al., 2009). Human echinococcosis is caused by the larval stage of *Echinococcus* spp. The two most important forms of this disease are cystic echinococcosis, caused by species of the complex *Echinococcus granulosus sensu lato* (*s.l.*) -that includes *Echinococcus granulosus sensu stricto* (*s.s.*) and *Echinococcus canadensis*, and alveolar echinococcosis caused by *Echinococcus multilocularis*. Cysticercosis is caused by the larvae (cysticerci) of *Taenia solium*. Treatment with anthelmintic drugs - benzimidazoles such as albendazole (ABZ) and praziquantel (PZQ) - is usually prolonged and often only partially effective (Hemphill et al., 2014; Gottstein et al., 2015). These drugs, in addition, are not well tolerated by some patients (Kyung et al., 2011; Lee et al., 2011). Therefore, the search for new, safe and highly effective cestocidals is imperative.

Targeting regulatory processes essential for parasite growth and development such as chromatin structure regulation and gene expression represents a promising starting point for identifying drug target candidates. In previous work, we identified and characterized HDAC-encoding genes in several cestode species (Vaca et al., 2019). Furthermore, we showed that the inhibition of these enzymes by several HDAC inhibitors (including both clinically approved and recently developed selective HDAC inhibitors) decreased parasite viability and induced alterations in the tegument and ultrastructural structures in the larval stage (tetrathyridium) of the laboratory model of cestodes *Mesocestoides vogae* (syn. *Mesocestoides corti*), suggesting their potential as drug targets (Vaca et al., 2019, 2021). Thus, studying the enzymes implicated in the regulation of chromatin structure and gene expression represents a promising avenue toward developing novel cestocidals. In spite of this, information about SIRTs in cestodes is very scarce. Previously, the presence of SIRT1-3 and SIRT6-7 orthologs were reported in the genomes of *E. granulosus s.s.* G1 and *E. multilocularis* (Lancelot et al., 2015). Furthermore, high expression of SIRT1 and SIRT2 was reported in metacestodes and protoscoleces of *E. granulosus s.s.*, as well as up-regulation of SIRT3

in metacestodes with respect to protoscoleces (Loos et al., 2018). More information is needed in order to analyze the role of SIRTs in cestodes and their potential as drug targets.

This study aimed to identify and characterize SIRTs in several cestode species and to study the cestocidal properties of several SIRT inhibitors in the laboratory model of cestode *M. vogae*. The identification and characterization of SIRTs should help to explore their roles in cestodes and to aid in the development of new treatments against NTDs caused by these parasites.

2. Materials and methods

2.1. Ethics statement

Experiments involving the use of experimental animals were conducted strictly in accordance with the protocols approved by the Comité Institucional para el Cuidado y Uso de Animales de Laboratorio (CICUAL), Facultad de Medicina, Universidad de Buenos Aires (UBA), Argentina (protocols: "*In vivo* passages of cestode parasites from *Mesocestoides vogae*" CD N° 1127/2015 and "Histone modifying enzymes in flatworms: study of their potential as new drug targets in diseases of importance in veterinary medicine and human health" CD N° 187/2020).

2.2. Parasite material

The *M*. *vogae* tetrathyridia (TTy) used in this work were maintained in the laboratory by alternate intraperitoneal infection in Wistar rats and BALB/c mice, as described previously (Markoski et al., 2003). The experimental animals were bred and housed in a temperature-controlled light cycle room with food and water ad libitum at the animal facilities of Instituto de Investigaciones en Microbiología y Parasitología Médica (IMPaM), Universidad de Buenos Aires

(UBA) y Consejo Nacional de Investigaciones Científicas y Tecnológicas (CONICET), Ciudad Autónoma de Buenos Aires, Argentina. After 3 months of infection, mice were euthanized by CO_2 inhalation. TTy were collected from the peritoneal cavity, using standard aseptic techniques, and washed three times with sterile PBS solution, pH 7.2, with levofloxacin (20 µg/mL). Finally, before being employed in experiments, TTy were size-selected using monofilament polyester meshes to a final size of 150 to 250 µm and incubated for 24 h in 5 mL of MvRPMI medium -a modified RPMI 1640 medium without phenol red (Sigma-Aldrich, USA) complemented with 10% v/v inactivated fetal bovine serum (INTERNEGOCIOS SA, Argentina), 2.4 g/L of HEPES Free acid (JT Baker, USA), 2.5 g/L of glucose (4,5 g/L final concentration, Britania, Argentina), 2 g/L of Sodium Bicarbonate (Anedra, Argentina), 20 µg/mL of levofloxacin (Tavanic, SANOFI, Argentina) and 1% v/v Pen/Strep (Penicillin-Streptomycin 10,000 U/mL, Gibco, USA)- at 37°C under 5% CO_2 atmosphere.

2.3. Bioinformatics analyses

Cestode genomes and predicted proteomes used in this work, from WormBase ParaSite database version: WBPS15.0 (Howe et al., 2016, 2017), were selected according to reported parameters of Core Eukaryotic Genes Mapping Approach (CEGMA) (>90%) and the N_{50} statistic (defined as the shortest contig length that needs to be included for covering 50% of the genome) (>5 Kb): *E. canadensis* G7 (*Ec*), *E. granulosus s.s.* G1 (*Eg*), *E. multilocularis* (*Em*), *M. vogae* (*Mv*) and *T. solium* (*Ts*) (Supplementary Table S1). SIRT-encoding genes were initially identified in the predicted cestode proteomes by BLASTP searches, using as a query the canonical amino-acid sequences of SIRT1-7 genes from *Homo sapiens* and an E-value ≤ 0.00001. The results obtained by this analysis were complemented by TBLASTN searches in cestode genomes, the use of the gene predictor programs Augustus (Hoff and Stanke, 2013) and FGENESH+ (Solovyev, 2007), and the use of the general tool for pairwise sequence comparison, Exonerate (Slater and Birney, 2005). Finally,

for each putative SIRT-encoding gene model identified in cestode genomes, reciprocal BLASTP searches were performed against the *H. sapiens* proteome (https://www.uniprot.org/proteomes/UP000005640).

Phylogenetic analyses were performed to determine the evolutionary relationships of cestode SIRT proteins to define classes and family. For these analyses, we included SIRT proteins from the model species *H*. *sapiens* (Hs)*, Mus musculus* (*Mm*), *Drosophila melanogaster* (*Dm*), and *S*. *mansoni* (*Sm*). Evolutionary analyses were conducted in MEGAX (Kumar et al., 2018). First, conserved SIRT catalytic domains (Pfam Family: PF02146) were identified by sequence analysis, using profile hidden Markov models (HMMER) and the profile database Pfam, and then aligned by the programs ClustalW and Muscle integrated packages in MEGAX. The alignment of sequences was adjusted by manual edition when necessary. The phylogenetic trees were inferred using the Maximum Likelihood method based on the JTT matrix-based model and the Neighbour-joining method based on a Poisson correction substitution model. The bootstrap consensus trees were inferred from 1000 replicates. These analyses involved 50 SIRT catalytic domain amino acid sequences. All positions with less than 95% site coverage were eliminated. There was a total of 99 positions in the final dataset. Finally, each cestode SIRT catalytic domain was compared with those from humans by Clustal2.1, to determine the percentages of identity.

2.4. Expression analyses of SIRT-encoding genes in Echinococcus spp.

Transcriptional expression levels for SIRT-encoding genes were determined using available RNAseq data from *E*. *granulosus s.s*. G1 (Zheng et al., 2013) and *E*. *multilocularis* (Huang et al., 2016). The expression level for each SIRT gene, expressed in reads per kilobase million mapped reads (RPKM), was compared among the different developmental stages: protoscoleces (PSC),

germinal and laminated layers -or cyst wall (CW)-, oncospheres (Onc) and adults for *E. granulosus s.s.* G1. and Onc, activated Onc (Act Onc), 4 week metacestode miniature vesicles (4wCW) and metacestode small vesicles cultivated in vitro (Cmet) for *E. multilocularis*.

2.5. Compounds

The SIRT inhibitors used in this work, AGK2, EX-527, Mz236, and Mz25, are shown in Fig. 1. Mz236 and Mz25 were synthesized and purified as described previously (Rumpf et al., 2015). AGK2 was purchased from Sigma (Germany) and EX527 from Tocris (Germany). ABZ was purchased from Sigma-Aldrich (USA). All stock solutions were prepared at 10 mM in 100% dimethylsulfoxide (DMSO) and stored at -20°C until use.

2.6. In vitro anthelmintic assays

In order to determine the in vitro effect of each SIRT inhibitor on parasite viability, the motility assay was employed with a worm tracker device (WMicrotracker Designplus SRL, Argentina) that was previously adapted to measure the movement of *M. vogae* TTy (Camicia et al., 2018; Vaca et al., 2019, 2021). Briefly, five TTy per well were incubated in U-shaped 96-well microplates (Greiner Bio-One, Germany) with 200 µL of MvRPMI medium at 37°C under 5% CO_2 atmosphere for 9 days without changing the medium. SIRT inhibitors were tested at concentrations of 2, 20 and 50 µM. Parasites pre-treated with ethanol 70% for 30 min or ABZ at 20 µM were used as positive controls. All motility assays were performed using an equal amount of the drug vehicle (1% DMSO final concentration) and the corresponding negative control (1% DMSO). Additionally, parasite cultures were inspected daily in order to determine any possible

morphological alterations in TTy treated with the compounds. Images were taken using a digital video camera (AxioCam ERc5c, Carl Zeiss, Germany) coupled to an inverted microscope (Primo Vert, Carl Zeiss, Germany).

Phenotypic screening data were collected from three independent biological replicates, each corresponding to TTy obtained from a different mouse, in quadruplicate for each tested condition. Relative motility indices were determined as described previously (Camicia et al., 2018; Vaca et al., 2019, 2021). Statistical analyses were carried out using GraphPad Prism 8.0.2. Two-way ANOVA tests were used to analyze the effects of the compounds on parasite viability. Significant differences ($P < 0.05$) were determined by Dunnett's comparisons post-tests, comparing each compound concentration with the negative controls (each run on each day).

2.7. Evaluation of dose-dependent effect and irreversibility test

Dose-dependent and irreversibility effects on parasite viability were determined in vitro for SIRT inhibitors using the *M. vogae* TTy motility assay (described in section 2.6). For dose-dependent effect determination, SIRT inhibitors were tested at concentrations ranging from 2 µM to 50 µM and relative motility indices were determined after 6 days of treatment. The half-maximal (IC_{50}), 90% (IC_{90}), and 25% (IC_{25}) inhibitory concentration values were determined from dose-dependent curves generated by non-linear regression analysis using GraphPad Prism 8.0.2. Additionally, one-way ANOVA tests were used for statistical analysis of differences in IC_{50} values. Significant differences ($P < 0.05$) were determined by Dunnett's comparison post-tests, comparing the IC_{50} determined for SIRT inhibitors with that determined for ABZ under the same conditions. For the irreversibility test, TTy were incubated with the compounds at IC_{90} concentrations. After 6 days of treatment, the culture medium was removed and TTy were gently washed four times in

PBS at 37°C. Then, washed TTy were incubated for 8 additional days in a fresh culture medium without adding the compounds. Relative motility indices were determined every day. For both assays, data were collected from three independent biological replicates, each corresponding to TTy obtained from a different mouse, in quadruplicate for each tested condition.

2.8. Scanning electron microscopy

To determine the effect of SIRT inhibitors on the tegument and parasite morphology at the ultrastructural level, TTy were processed for scanning electron microscopy (SEM) as was previously described (Maggiore and Elissondo, 2014; Vaca et al., 2021). Briefly, TTy were incubated with compounds at 20 µM. After 6 days of treatment, TTy were washed four times in PBS and fixed with 3% glutaraldehyde in phosphate buffer 0.1 M (PB), pH 7.4, for 72 h at 4°C. The samples were then washed four times in PB and dehydrated by sequential incubations in increasing concentrations of ethanol (50–100%). Finally, TTy were immersed in hexamethyldisilazane for 5 min, 1 h, and overnight, and then sputter-coated with gold (100 Å thick). Parasites incubated with 1% DMSO were used as a negative control. The samples were inspected and images were taken using a JEOL JSM-6460 LV scanning electron microscope operating at 15 kV.

2.9. Structure homology modeling

Protein structure models were performed for cestode SIRT2s by the SWISS-MODEL server (Arnold et al., 2006; Benkert et al., 2008; Biasini et al., 2014). For all sequences, crystallized structures of SIRT2 from *H. sapiens* (*Hs*SIRT2: PDB-IDs 4RMG and 4RMI) (Rumpf et al., 2015) were used as templates. All structure models obtained here were validated by calculating several

parameters. In this fashion, we used ERRAT program (an empirical atom-based method for validating protein structures) (Colovos and Yeates, 1993) (https://servicesn.mbi.ucla.edu/ERRAT/), the Qualitative Model Energy Analysis (QMEAN) and Ramachandran plots (https://swissmodel.expasy.org/assess). Also, the Root-Mean-Square Deviation (RMSD) and TM-align algorithm (Zhang and Skolnick, 2005) (https://zhanglab.ccmb.med.umich.edu/TM-align/) were used to compare the structure of models obtained here to *Hs*SIRT2. Structural comparisons were performed to identify relevant and conserved residues in ion and cofactor binding sites, as well as in inhibitor-interaction site. The molecular visualization and figures generated in this work were performed using the PyMOL Molecular Graphics System, Version 2.0.4 Schrödinger, LLC).

3. Results

3.1. Classes I, III and IV SIRT-encoding genes were identified in cestode genomes

In an initial analysis, we searched for SIRT-encoding genes in the draft predicted proteomes of the cestodes: *E*. c*anadensis* G7, *E*. *granulosus s.s.* G1, *E*. *multilocularis*, *M*. *vogae* and *T*. *solium*, by BLASTP using the canonical SIRT1-7 from *H. sapiens* as a query. Although this first approach allowed identification of putative orthologs of human SIRTs, some of the genes were longer and/or contained more exons than expected and/or additional domains not corresponding to the SIRT catalytic domain. In the case of SIRT7, we found incomplete SIRT catalytic domains for all putative orthologs of human SIRT7 identified in cestode proteomes. Thus, we manually curated and re-annotated several SIRT-encoding genes by using gene prediction programs trained with *S*. *mansoni* genes (see Supplementary Data S1 for a detailed description of SIRT-encoding gene annotation). As a result, we identified five proteins corresponding to SIRT enzymes in the genomes of *E*. *canadensis* G7, *E*. *multilocularis*, and *T*. *solium*; while six SIRT proteins were found in the

genomes of *E. granulosus* s. s G1 and *M. vogae*. All SIRT-encoding genes identified here are shown in Table 1, each with its protein size in amino acids, the coding DNA sequence (CDS) localization and the closest human ortholog. In Supplementary Data S1 also are shown the sequences for CDSs, exons, proteins and genome regions for the SIRT-encoding genes re-annotated here. All analyses carried out here were performed on the basis of these predicted genes.

To determine the evolutionary relationships of cestode SIRT proteins identified here and define the classes they belong to, phylogenetic analyses of conserved SIRT catalytic domains were carried out. A phylogenetic tree model obtained by the Neighbor-joining method is shown in Fig. 2. Similar results were obtained by the Maximum Likelihood method (data not shown). We found that all cestodes analyzed here showed an ortholog of the mammalian SIRT1, SIRT2, and SIRT3 (Class I), and of SIRT6 and SIRT7 (Class IV) and, only in *E. granulosus s.s.* G1 and *M. vogae*, a mammalian SIRT5 (Class III) ortholog. These genes are also orthologs of SIRT5 from *S. mansoni* (a parasite included for these analyses). No mammalian SIRT4 (class II) ortholog was found among cestode SIRT proteins. We also found that cestode SIRT proteins from different species of the same genus grouped together.

We compared the level of amino acid identity of cestode SIRT catalytic domains with those from human SIRT proteins to identify potential selective drug targets. We found that all cestode SIRT proteins showed a high level of amino acid conservation to SIRT catalytic domains (Fig. 3), with identities ranging from 46.84% to 72.46%. SIRT catalytic domains from cestode SIRT1s showed the highest similarity to *Hs*SIRT1 with identities above 65.24%; while those of cestode SIRT7s showed the lowest similarity to *Hs*SIRT7 with identities of 46.84% to 56.25%.

3.2. SIRT genes showed transcriptional expression in several developmental stages of Echinococcus spp.

As was revealed by RNA-seq data analysis, we found that all SIRT-encoding genes showed transcriptional expression in at least one developmental stage in *E. granulosus s.s.* G1 and *E. multilocularis* (Fig. 4), with SIRT2-encoding genes being the most expressed in all analyzed developmental stages for both *Echinococcus* spp. For *E. granulosus* s.s. G1, *Eg*SIRT5 and *Eg*SIRT6 genes also showed transcriptional expression in all analyzed developmental stages: Adult, Onc, PSC, and CW. *Eg*SIRT1 showed expression in adult worms and hydatid cyst-related PSC and CW stages but not in Onc; while *Eg*SIRT3 and *Eg*SIRT7 did not show detectable expression in Onc or PSC stages (Fig. 4A). For *E. multilocularis*, *Em*SIRT1 and *Em*SIRT6 genes also showed transcriptional expression in all analyzed developmental stages: Onc, Act Onc, 4wCW, and Cmet; while no detectable expressions were observed in 4wCW or Cmet for *Em*SIRT3 or in 4wCW for *Em*SIRT7 (Fig. 4B).

3.3. The SIRT inhibitor Mz25 showed high cestocidal activity in Mesocestoides vogae tetrathyridia

We determined the in vitro cestocidal activity of the SIRT inhibitors AGK2, EX-527, Mz236, and Mz25 by the *M. vogae* TTy motility assay and inverted optical microscope observations (Fig. 5). Of them, we found that the selective SIRT2 inhibitor Mz25 showed inhibitory properties with a strong cestocidal activity in a time- and dose-dependent manner (Fig. 5D and E). Mz25 showed a significant reduction in TTy viability at 50 µM (14.7%; $P < 0.0001$) and at 20 µM (25.6%; $P < 0.0001$) after 1 and 5 days of treatment, respectively, and killed all TTy (reducing parasite viability by 100%) at 50 µM and 20 µM after 6 and 9 days of treatment; respectively (Fig. 5D). Furthermore, Mz25 induced extensive damage to the tegument with general morphological alterations,

compared with untreated TTy, as revealed by inverted optical microscopy observations (Fig. 5E). Needle-like structures were observed in the tegument of TTy incubated with Mz25 at 50 μM and 20 μM after 2 days of treatment. Additionally, extensive damage to the tegument and other morphological alterations were observed in TTy treated with Mz25 at 50 μM and 20 μM, compared with TTy incubated with DMSO at 1% or Mz25 at 2 μM (Fig. 5E). The main changes observed were the presence of influx of culture medium into the worms and blebs in the tegument, as well as tegumental debris in the culture medium. Furthermore, we did not observe significant effects on parasite viability or morphology in TTy treated with the other SIRT inhibitors AGK2, EX-527, or Mz236 at any tested concentrations, even after up to 9 days of treatment, compared with untreated parasites (Fig. 5A, B and C, respectively).

3.4. The SIRT inhibitor Mz25 showed dose-response and irreversible cestocidal activity in Mesocestoides vogae tetrathyridia

We found that Mz25 showed a dose-response cestocidal activity with values for the dose-response relationship (IC_{25}, IC_{50}, and IC_{90}) in the micromolar range (Table 2). Under the same assay conditions, we determined an IC_{50} value for Mz25 (17.20 ± 2.62 μM, $P < 0.05$), which was significantly lower than that of ABZ (20.58 ± 0.38 μM) (Vaca et al., 2021). Furthermore, we assessed the irreversibility of the in vitro cestocidal activity of Mz25 (Fig. 6). We found that Mz25 showed cestocidal activity in a time-dependent manner when tested at its IC_{90} concentration, similar to the irreversible cestocidal activity determined for ABZ under the same assay conditions. The *M. vogae* TTy viability determined for Mz25 at 6 days of treatment was close to that expected, considering that this compound was tested at its IC_{90} value. The effect observed for Mz25 was not reversed after removing this compound from the culture medium and, even after 10 days of

incubation, the reduction of *M. vogae* TTy viability reached 100% (Fig. 6). All numerical data determined in this and previous sections of this study are shown in Supplementary Table S2.

3.5. The SIRT inhibitor Mz25 induced large morphological alterations in Mesocestoides vogae tetrathyridia

By SEM studies we found that Mz25 induced extensive damage in the general morphology of *M. vogae* TTy with marked alterations in the tegument and ultrastructural features (Fig. 7). The main changes we observed in Mz25-treated parasites were extensive erosion in the tegument and general morphological disintegration (Fig. 7D-F). However, it was not possible to distinguish the needle-like structures observed by inverted optical microscopy (see section 3.3 and Fig. 5E), possibly due to the several steps of fixing, washing and dehydration for SEM preparations. However, we observed some areas with a large aggregation of tegument eruption that could be the base of the needle-like structure. In more detailed images of the tegument of treated TTy, we also observed a large number of vesicle-like structures of different sizes and complete loss of microtriches (Fig. 7F). These phenotypic effects were not observed in TTy incubated with the drug vehicle, 1% DMSO, used as a negative control (Fig. 7A-C).

3.6. Cestode SIRT2s showed the canonical SIRT structure

We characterized cestode SIRT2s to determine if these proteins share structural differences with respect to *Hs*SIRT2 (Fig. 8). The alignment of the SIRT catalytic domain amino acid sequences of SIRT2s from cestodes, human (*Hs*SIRT2) and *S. mansoni* (*Sm*SIRT2) is shown in Fig. 8A. We found that cestode SIRT2 proteins exhibited a major conservation in their amino acid

sequences of SIRT catalytic domains with respect to *Hs*SIRT2 and *Sm*SIRT2. In cestode SIRT2s, we found a deletion, also present in *Sm*SIRT2, and an insertion of two amino acid residues not shared with *Hs*SIRT2. No mutations were found in cestode SIRT2s for the residues implicated in zinc coordination (Fig. 8A and Supplementary Fig. S1) or NAD^+ cofactor binding, except for the residues I169 and K287 in *Hs*SIRT2 which are conservatively replaced by a valine and an arginine residue, respectively. By homology modeling, we found that all cestode SIRT2s showed the canonical SIRT structure (Fig. 8B), composed of a two-domain structure: the larger NAD^+ domain with a Rossmann fold (six parallel β-strands sandwiched between two layers of α-helices) and a smaller zinc-binding domain, both separated through a large groove that constitutes the active site. Ramachadran plots of all homology models obtained here showed that more than 93.42% of residues were in favored regions, while more than 99.75% of residues were in allowed regions and only 0.66% of residues were in outlier regions (Supplementary Table S3 and Supplementary Figs. S2-S6). In addition, we obtained ERRAT values above 86.0544 and QMEAN values ranging from -2.88 to -2.46 for all these models (Supplementary Table S3), indicating the good quality of the models. Furthermore, we obtained RMSD values below 0.73 Å and TM-align values above 0.97070 for all cestode SIRT2 homology models compared with *Hs*SIRT2, suggesting the same fold for cestode SIRT2 proteins and a good overlap amongst these proteins (Supplementary Table S3). Assuming that Mz25 binds to cestode SIRT2s in a similar fashion as observed for *Hs*SIRT2, we found good conservation of residues implicated in Mz25 binding. Only the residues L134, I169, and I232 in *Hs*SIRT2, which interact with the naphthyl moiety of Mz25, are conservatively replaced by valine residues in cestode SIRT2s (Fig. 8C). However, the residues P140, F143, and L206 in the selectivity pocket of *Hs*SIRT2 - the region of the binding pocket that is formed by induction of the dimethylmercaptopyrimidine substituent of Mz25 (Rumpf et al., 2015) - are replaced by arginine, alanine, and phenylalanine residues, respectively.

4. Discussion

In this study we describe the full repertoire of SIRT-encoding genes in several cestode species from *Echinococcus*, *Mesocestoides* and *Taenia* genera. After detailed inspection of putative SIRT orthologs and re-annotation of several SIRT-encoding genes, we identified three Class I (SIRT1, SIRT2, and SIRT3) and two Class IV (SIRT6 and SIRT7) SIRT-encoding genes in the genomes of *E. canadensis* G7, *E. granulosus s.s.* G1, *E. multilocularis*, *M. vogae,* and *T. solium*. Our results confirm the previous report of SIRT-encoding genes in *E*. *granulosus s.s.* G1 and *E*. *multilocularis* genomes (Lancelot et al., 2015) and extend SIRT genomic information to the zoonotic cestodes *E*. *canadensis* G7 and *T*. *solium,* and to the laboratory model of cestodes *M*. *vogae*. Furthermore, we identified a SIRT Class III (SIRT5) in one of the available genomes of *E. granulosus s.s.* G1 (*Eg*SIRT5) (Zheng et al., 2013) and in the *M*. *vogae* (*Mv*SIRT5) genome. Our analysis revealed that these SIRT5 genes display conserved SIRT catalytic domains for amino acid sequences. Most importantly, we found transcriptional expression for *Eg*SIRT5 in all analyzed developmental stages, suggesting that these genes may be encoding a functional SIRT5 enzyme. The absence of SIRT5-encoding genes in the remaining cestode genomes of *E*. *canadensis* G7, *E*. *multilocularis* and in the other available genome of *E. granulosus s.s.* G1 (Tsai et al., 2013), could be due to incompleteness of genome assemblies or annotations. These genomes were assembled and annotated based on the *E. multilocularis* reference genome (Tsai et al., 2013), in which only a fragment with a very low identity with *Eg*SIRT5 or *Mv*SIRT5 was identified. We did not identify any SIRT4-encoding genes (Class II) in the analyzed cestode genomes. Class II SIRT genes were reported in vertebrates and ecdysozoans such as *D*. *melanogaster*, but not in Plathyhelminths. In the case of the nematode *Caenorhabditis elegans*, two orthologs of Class II SIRT genes were reported, sir-2.2 and sir-2.3, with the characteristic conserved region (RQRYWAR) of the SIRT4 enzymes (Anderson et al., 2017). Finally, our results are in agreement with those previously reported in three *Schistosoma* spp.: *S*.

mansoni, *Schistosoma japonicum* and *Schistosoma haematobium* (Lancelot et al., 2013, 2015; Scholte et al., 2017). In these parasites, SIRT-encoding genes belonging to Classes I (SIRT1 and SIRT2), III (SIRT5), and IV (SIRT6 and SIRT7) were identified, but not Class II. However, here we identified a gene encoding SIRT3 (Class I) in all analyzed cestode genomes that was not described for S*chistosoma* spp. SIRT3 genes were also previously reported in *E*. *granulosus s.s.* G1 and *E*. *multilocularis* (Lancelot et al., 2015), as well as their presence and expression (together with SIRT1 and SIRT2) in *E*. *granulosus s.s.* larval stages (Loos et al., 2018); but no information was available for other cestodes.

By transcriptional data analyses, we revealed that several SIRT-encoding genes are expressed in each developmental stage of *E*. *granulosus s.s.* G1 and *E*. *multilocularis*, suggesting that SIRTs are important for parasite development and/or maintenance of the particular features of each stage. All SIRT genes were expressed in at least one stage of both parasites, providing transcriptional evidence for our bioinformatic predictions. In particular, SIRT2 was expressed in all developmental stages of both parasites and displayed the highest expression level in comparison to the other SIRT genes, suggesting an important role for parasite biology. In *E*. *multilocularis*, *Em*SIRT1 was also highly expressed in all analyzed developmental stages. The wide expression of SIRT genes found in this study is in line with mammalian SIRT roles in multiple cellular processes including cellular stress resistance, genomic stability, tumorigenesis and energy metabolism (Finkel et al., 2009).

We also analyzed the cestocidal activity of several SIRT inhibitors using *M*. *vogae* TTy. This laboratory model of cestodes has been widely used to identify new cestocidals in pharmacological studies (Hrčková et al., 1998; Markoski et al., 2006; Maggiore and Elissondo, 2014; Vaca et al., 2021) since it is easily cultured, non-infective for humans and has a remarkable capacity for asexual reproduction in the peritoneal cavity of mice, providing a continuous availability of

biological material (Thompson et al., 1982; Hrčková et al., 1998), an important limitation in the work with cestodes. Using a *M*. *vogae* TTy motility assay, here we determined the cestocidal activity of the SIRT inhibitors EX-527 (Napper et al., 2005), AGK2 (Outeiro et al., 2007), and the aminothiazole derivatives Mz236 (SirReal1) and Mz25 (SirReal2) (Rumpf et al., 2015; Schiedel et al., 2016). The indol EX-527 is a potent and selective inhibitor of *Hs*SIRT1. The remaining SIRT inhibitors are selective inhibitors of *Hs*SIRT2. In particular, Mz25 showed high potency and selectivity towards *Hs*SIRT2. The IC_{50} of Mz25 to *Hs*SIRT2 is 0.4 μM and has very little effect on the activities of SIRT3-5. Only at higher concentrations (100-200 μM) is Mz25 able to produce partial (~20%) inhibition on *Hs*SIRT1 and *Hs*SIRT6, making Mz25 one of the most selective SIRT2 inhibitors (Rumpf et al., 2015). Furthermore, Mz25 belongs to SIRT-rearranging ligands (named SirReals) that induce a structural rearrangement of the active site, allowing exploitation of an adjacent binding pocket (Rumpf et al., 2015). In this work, we showed that Mz25 displayed strong, irreversible and time- and dose-dependent in vitro cestocidal activity, comparable to the current anthelmintic drug ABZ. This finding was validated by inverted optical microscopy observations of Mz25-treated parasites. We also observed an evident alteration of general morphology and damage to the tegument that is an important parasite structure involved in nutrient digestion and absorption (cestodes lack a digestive tract) (Dalton et al., 2004), parasite protection and modulation of the host immune response (Littlewood, 2006). Interestingly, needle-like structures were apparent in the tegument of treated parasites. To date, this alteration was not observed previously by treating the parasite with the current anthelmintic drugs ABZ or PZQ and novel compounds such as thymol or HDAC inhibitors (Hrčková et al., 1998; Maggiore and Elissondo, 2014; Fabbri and Elissondo, 2019; Vaca et al., 2021, 2019). Although we do not know the reason why these structures are present, we speculate that they could be related to an alteration of tubulin polymerization, since in humans SIRT2 is involved in alpha-tubulin acetylation (Outeiro et al., 2007). Further experiments will be conducted in the future to determine if SIRT2 plays the same function in cestodes. The

analysis of the impact of Mz25 at the ultrastructural level revealed a general alteration of parasite morphology with large areas with complete erosion of the tegument, the presence of vesicle-like structures of different sizes and a general loss of microtriches. Microtriches are cytoplasmic extensions that significantly augment the parasite surface, thus allowing nutrient absorption from the host milieu. Loss of these structures would probably be detrimental for *M*. *vogae* by interfering with nutritional uptake. Phenotypic alterations observed by SEM in Mz25-treated parasites were similar to those observed in *M*. *vogae* TTy treated with PZQ (Hrčková et al., 1998), thymol (Maggiore and Elissondo, 2014; Fabbri and Elissondo, 2019), or HDAC inhibitors (Vaca et al., 2021). These results suggest that Mz25 is a promising compound for further evaluation towards the development of new cestocidals. Nevertheless, at this stage the Mz25 molecular target in *M. vogae* is unknown and remains to be determined.

Although the Mz25 molecular target in *M. vogae* is still unknown, we think that the effect of Mz25 on parasite viability could be due to inhibition of its SIRTs, particularly SIRT2, as observed in *H. sapiens* for *Hs*SIRT2 (Rumpf et al., 2015). Considering this reasoning and due to the strong cestocidal activity of Mz25, we focused on cestode SIRT2 for further analysis. SIRT2 genes also showed transcriptional expression in all analyzed developmental stages of *E*. *granulosus s.s.* G1 and *E*. *multilocularis*, being the most expressed SIRT in all analyzed developmental stages for both *Echinococcus* spp. By homology modeling, we found conservation of the canonical SIRT structure for cestode SIRT2s. Analysis of the catalytic sites of these proteins revealed conservation of residues involved in zinc coordination (located at the N-acetyl lysine channel) and in NAD^+ cofactor binding (at the C-pocket of the active site). Furthermore, assuming that Mz25 binds to cestode SIRT2s in a similar fashion as observed for *Hs*SIRT2, we found high conservation of residues related to Mz25-SIRT2 binding (at the extended C-pocket of the catalytic site), suggesting that Mz25 might inhibit cestode SIRT2s. Interestingly, some non-conservative mutations were found in cestode SIRT2s on the selectivity pocket, a rearrangement induced by Mz25 binding (Rumpf et al., 2015).

This last finding represents a promising point for developing Mz25 derivatives that can have both more selectivity for cestode enzymes, and similar or higher efficacy to alter parasite motility and morphology. However, it is necessary to determine the effect of Mz25 on parasite SIRT2 activity in order to experimentally validate these predictions.

The results obtained in the present study lay a foundation for the search of parasite-selective SIRT inhibitors. Recently, compound library screening and further structure-activity relationship analysis of selected hits led to the synthesis of *Sm*SIRT2 inhibitors that decreased *S. mansoni* juvenile and adult worm viability with no toxicity in human cancer cell lines (Monaldi et al., 2019). Similar studies could be conducted in the future to identify selective cestode SIRT inhibitors.

This report paves the way for further studies on cestode SIRT structure and activity as well as the identification of new selective SIRT inhibitors for the treatment of neglected cestode diseases.

Acknowledgments

We would like to thank Eduardo Giménez from the Instituto de Investigaciones en Microbiología y Parasitología Médica (IMPaM), Facultad de Medicina, Universidad de Buenos Aires (UBA, Argentina, for his excellent technical assistance. This work was supported by the Agencia Nacional de Promoción Científica y Tecnológica, Argentina (grant numbers PICT 2017 N° 2966 and PICT 2019 N°3367), Secretaría de Ciencia y Técnica; Universidad de Buenos Aires (UBACyT), Argentina (grant number N° 20020190100230BA). H.R.V. and M.A.T. are recipients of Consejo Nacional de Investigaciones Científicas y Técnicas (CONICET), Argentina, post-doctoral and

doctoral fellowships. A-T.H and M.J. thank the Deutsche Forschungsgemeinschaft (DFG), Germany, for funding (CRC992 (Project: ID192904750), Ju 295/14-1 and GRK1976 Project ID 235777276).

References

Anderson, K.A., Huynh, F.K., Fisher-Wellman, K., Stuart, J.D., Peterson, B.S., Douros, J.D., Wagner, G.R., Thompson, J.W., Madsen, A.S., Green, M.F., Sivley, R.M., Ilkayeva, O.R., Stevens, R.D., Backos, D.S., Capra, J.A., Olsen, C.A., Campbell, J.E., Muoio, D.M., Grimsrud, P.A., Hirschey, M.D., 2017. SIRT4 is a Lysine Deacylase that Controls Leucine Metabolism and Insulin Secretion. Cell Metab. 25, 855.e15. https://doi.org/10.1016/J.CMET.2017.03.003

Arnold, K., Bordoli, L., Kopp, J., Schwede, T., 2006. The SWISS-MODEL workspace: a web-based environment for protein structure homology modelling. Bioinformatics 22, 195–201. https://doi.org/10.1093/bioinformatics/bti770

Benkert, P., Tosatto, S.C.E., Schomburg, D., 2008. QMEAN: A comprehensive scoring function for model quality assessment. Proteins Struct. Funct. Bioinforma. 71, 261–277. https://doi.org/10.1002/prot.21715

Biasini, M., Bienert, S., Waterhouse, A., Arnold, K., Studer, G., Schmidt, T., Kiefer, F., Cassarino, T.G., Bertoni, M., Bordoli, L., Schwede, T., 2014. SWISS-MODEL: modelling protein tertiary and quaternary structure using evolutionary information. Nucleic Acids Res. 42, W252–W258. https://doi.org/10.1093/nar/gku340

Budke, C.M., White, A.C., Garcia, H.H., 2009. Zoonotic Larval Cestode Infections: Neglected, Neglected Tropical Diseases?. PLoS Negl. Trop. Dis. 3(2), e319. https://doi.org/10.1371/journal.pntd.0000319

Camicia, F., Celentano, A.M., Johns, M.E., Chan, J.D., Maldonado, L., Vaca, H., Di Siervi, N., Kamentezky, L., Gamo, A.M., Ortega-Gutierrez, S., Martin-Fontecha, M., Davio, C., Marchant, J.S., Rosenzvit, M.C., 2018. Unique pharmacological properties of serotoninergic G-protein coupled receptors from cestodes. PLoS Negl. Trop. Dis. 12, e0006267.

https://doi.org/10.1371/journal.pntd.0006267

Colovos, C., Yeates, T.O., 1993. Verification of protein structures: Patterns of nonbonded atomic interactions. Protein Sci. 2, 1511–1519. https://doi.org/10.1002/pro.5560020916

Dalton, J.P., Skelly, P., Halton, D.W., 2004. Role of the tegument and gut in nutrient uptake by parasitic platyhelminths. Can. J. Zool. 82, 211–232. https://doi.org/10.1139/Z03-213

Fabbri, J., Elissondo, M.C., 2019. Comparison of different staining methods for determination of viability on *Mesocestoides vogae* tetrathyridia. Parasitol. Res. 118, 687–692. https://doi.org/10.1007/s00436-018-6143-9

Finkel, T., Deng, C.-X., Mostoslavsky, R., 2009. Recent progress in the biology and physiology of sirtuins. Nature 460, 587–591. https://doi.org/10.1038/NATURE08197

Fioravanti, R., Mautone, N., Rovere, A., Rotili, D., Mai, A., 2020. Targeting histone acetylation/deacetylation in parasites: an update (2017–2020). Curr. Opin. Chem. Biol. 57, 65-74. https://doi.org/10.1016/j.cbpa.2020.05.008

Frye, R.A., 2000. Phylogenetic Classification of Prokaryotic and Eukaryotic Sir2-like Proteins. Biochem. Biophys. Res. Commun. 273, 793–798. https://doi.org/10.1006/bbrc.2000.3000

Gottstein, B., Stojkovic, M., Vuitton, D.A., Millon, L., Marcinkute, A., Deplazes, P., 2015. Threat of alveolar echinococcosis to public health – a challenge for Europe. Trends Parasitol. 31, 407–412. https://doi.org/10.1016/j.pt.2015.06.001

Hemphill, A., Stadelmann, B., Rufener, R., Spiliotis, M., Boubaker, G., Müller, J., Müller, N., Gorgas, D., Gottstein, B., 2014. Treatment of echinococcosis: albendazole and mebendazole – what else? Parasite 21, 70. https://doi.org/10.1051/parasite/2014073

Hoff, K.J., Stanke, M., 2013. WebAUGUSTUS--a web service for training AUGUSTUS and predicting genes in eukaryotes. Nucleic Acids Res. 41, W123–W128. https://doi.org/10.1093/nar/gkt418

Howe, K.L., Bolt, B.J., Cain, S., Chan, J., Chen, W.J., Davis, P., Done, J., Down, T., Gao, S., Grove, C., Harris, T.W., Kishore, R., Lee, R., Lomax, J., Li, Y., Muller, H.-M., Nakamura, C., Nuin, P., Paulini, M., Raciti, D., Schindelman, G., Stanley, E., Tuli, M.A., Van Auken, K., Wang, D., Wang, X., Williams, G., Wright, A., Yook, K., Berriman, M., Kersey, P., Schedl, T., Stein, L., Sternberg, P.W., 2016. WormBase 2016: expanding to enable helminth genomic research. Nucleic Acids Res. 44, D774-80. https://doi.org/10.1093/nar/gkv1217

Howe, K.L., Bolt, B.J., Shafie, M., Kersey, P., Berriman, M., 2017. WormBase ParaSite - a comprehensive resource for helminth genomics. Mol. Biochem. Parasitol. 215, 2–10. https://doi.org/10.1016/j.molbiopara.2016.11.005

Hrčková, G., Velebný, S., Corba, J., 1998. Effects of free and liposomized praziquantel on the surface morphology and motility of *Mesocestoides vogae* tetrathyridia (syn. *M. corti*; Cestoda: Cyclophyllidea) *in vitro*. Parasitol. Res. 84, 230–238. https://doi.org/10.1007/s004360050387

Huang, F., Dang, Z., Suzuki, Y., Horiuchi, T., Yagi, K., Kouguchi, H., Irie, T., Kim, K., Oku, Y., 2016. Analysis on Gene Expression Profile in Oncospheres and Early Stage Metacestodes from *Echinococcus multilocularis*. PLoS Negl. Trop. Dis. 10, e0004634. https://doi.org/10.1371/journal.pntd.0004634

Kumar, S., Stecher, G., Li, M., Knyaz, C., Tamura, K., 2018. MEGA X: Molecular evolutionary genetics analysis across computing platforms. Mol. Biol. Evol. 35, 1547–1549. https://doi.org/10.1093/molbev/msy096

Kyung, S.Y., Cho, Y.K., Kim, Y.J., Park, J.-W., Jeong, S.H., Lee, J.-I., Sung, Y.M., Lee, S.P., 2011. A Paragonimiasis Patient with Allergic Reaction to Praziquantel and Resistance to Triclabendazole: Successful Treatment after Desensitization to Praziquantel. Korean J. Parasitol. 49, 73. https://doi.org/10.3347/kjp.2011.49.1.73

Lancelot, J., Cabezas-Cruz, A., Caby, S., Marek, M., Schultz, J., Romier, C., Sippl, W., Jung, M.,

Pierce, R.J., 2015. Schistosome sirtuins as drug targets. Future Med. Chem. 7(6), 765-782. https://doi.org/10.4155/fmc.15.24

Lancelot, J., Caby, S., Dubois-Abdesselem, F., Vanderstraete, M., Trolet, J., Oliveira, G., Bracher, F., Jung, M., Pierce, R.J., 2013. *Schistosoma mansoni* Sirtuins: Characterization and Potential as Chemotherapeutic Targets. PLoS Negl. Trop. Dis. 7, e2428. https://doi.org/10.1371/journal.pntd.0002428

Lee, J.-M., Lim, H.-S., Hong, S.-T., 2011. Hypersensitive reaction to praziquantel in a clonorchiasis patient. Korean J. Parasitol. 49, 273–5. https://doi.org/10.3347/kjp.2011.49.3.273

Littlewood, D.T.J., 2006. The evolution of parasitism in flatworms, in: Maule, A.G., Marks, N.J. (Eds.), Parasitic Flatworms: Molecular Biology, Biochemistry, Immunology and Physiology. CABI Publishing, Wallingford pp. 1- 36. https://doi.org/10.1079/9780851990279.0000

Loos, J.A., Nicolao, M.C., Cumino, A.C., 2018. Metformin promotes autophagy in Echinococcus granulosus larval stage. Mol. Biochem. Parasitol. 224, 61–70. https://doi.org/10.1016/J.MOLBIOPARA.2018.07.003

Maggiore, M., Elissondo, M.C., 2014. *In Vitro* Cestocidal Activity of Thymol on *Mesocestoides corti* Tetrathyridia and Adult Worms. Interdiscip. Perspect. Infect. Dis. 2014, Article ID 268135. https://doi.org/10.1155/2014/268135

Markoski, M.M., Bizarro, C. V, Farias, S., Espinoza, I., Galanti, N., Zaha, A., Ferreira, H.B., 2003. In vitro segmentation induction of *Mesocestoides corti* (Cestoda) tetrathyridia. J. Parasitol. 89, 27–34. https://doi.org/10.1645/0022-3395(2003)089[0027:IVSIOM]2.0.CO;2

Markoski, M.M., Trindade, E.S., Cabrera, G., Laschuk, A., Galanti, N., Zaha, A., Nader, H.B., Ferreira, H.B., 2006. Praziquantel and albendazole damaging action on *in vitro* developing *Mesocestoides corti* (Platyhelminthes: Cestoda). Parasitol. Int. 55, 51–61.

https://doi.org/10.1016/j.parint.2005.09.005

Monaldi, D., Rotili, D., Lancelot, J., Marek, M., Wössner, N., Lucidi, A., Tomaselli, D., Ramos-Morales, E., Romier, C., Pierce, R.J., Mai, A., Jung, M., 2019. Structure-Reactivity Relationships on Substrates and Inhibitors of the Lysine Deacylase Sirtuin 2 from *Schistosoma mansoni* (SmSirt2). J. Med. Chem. 62, 8733–8759. https://doi.org/10.1021/acs.jmedchem.9b00638

Napper, A.D., Hixon, J., McDonagh, T., Keavey, K., Pons, J.F., Barker, J., Yau, W.T., Amouzegh, P., Flegg, A., Hamelin, E., Thomas, R.J., Kates, M., Jones, S., Navia, M.A., Saunders, J.O., DiStefano, P.S., Curtis, R., 2005. Discovery of indoles as potent and selective inhibitors of the deacetylase SIRT1. J. Med. Chem. 48, 8045–8054. https://doi.org/10.1021/jm050522v

Outeiro, T.F., Kontopoulos, E., Altmann, S.M., Kufareva, I., Strathearn, K.E., Amore, A.M., Volk, C.B., Maxwell, M.M., Rochet, J.C., McLean, P.J., Young, A.B., Abagyan, R., Feany, M.B., Hyman, B.T., Kazantsev, A.G., 2007. Sirtuin 2 inhibitors rescue α-synuclein-mediated toxicity in models of Parkinson's disease. Science 317, 516–519. https://doi.org/10.1126/science.1143780

Rumpf, T., Schiedel, M., Karaman, B., Roessler, C., North, B.J., Lehotzky, A., Oláh, J., Ladwein, K.I., Schmidtkunz, K., Gajer, M., Pannek, M., Steegborn, C., Sinclair, D.A., Gerhardt, S., Ovádi, J., Schutkowski, M., Sippl, W., Einsle, O., Jung, M., 2015. Selective Sirt2 inhibition by ligand-induced rearrangement of the active site. Nat. Commun. 6, 6263. https://doi.org/10.1038/ncomms7263

Schiedel, M., Robaa, D., Rumpf, T., Sippl, W., Jung, M., 2018. The Current State of NAD $^{+}$ -Dependent Histone Deacetylases (Sirtuins) as Novel Therapeutic Targets. Med. Res. Rev. 38, 147–200. https://doi.org/10.1002/med.21436

Schiedel, M., Rumpf, T., Karaman, B., Lehotzky, A., Gerhardt, S., Ovádi, J., Sippl, W., Einsle, O., Jung, M., 2016. Structure-Based Development of an Affinity Probe for Sirtuin 2. Angew. Chemie Int. Ed. 55, 2252–2256. https://doi.org/10.1002/anie.201509843

Scholte, L.L.S., Mourão, M.M., Pais, F.S.-M., Melesina, J., Robaa, D., Volpini, A.C., Sippl, W., Pierce, R.J., Oliveira, G., Nahum, L.A., 2017. Evolutionary relationships among protein lysine deacetylases of parasites causing neglected diseases. Infect. Genet. Evol. 53, 175–188. https://doi.org/10.1016/j.meegid.2017.05.011

Slater, G.S.C., Birney, E., 2005. Automated generation of heuristics for biological sequence comparison. BMC Bioinform. 6, 31–31. https://doi.org/10.1186/1471-2105-6-31

Solovyev, V., 2007. Statistical Approaches in Eukaryotic Gene Prediction, in: Balding, D.J., Bishop, M., Cannings, C. (Eds.), Handbook of Statistical Genetics: Third Edition. Wiley-Interscience, p. 1616. https://doi.org/10.1002/9780470061619.ch4

Thompson, R.C.A., Jue Sue, L.P., Buckley, S.J., 1982. In vitro development of the strobilar stage of *Mesocestoides corti*. Int. J. Parasitol. 12, 303–314. https://doi.org/10.1016/0020-7519(82)90033-9

Tsai, I.J., Zarowiecki, M., Holroyd, N., Garciarrubio, A., Sanchez-Flores, A., Brooks, K.L., Tracey, A., Bobes, R.J., Fragoso, G., Sciutto, E., Aslett, M., Beasley, H., Bennett, H.M., Cai, J., Camicia, F., Clark, R., Cucher, M., De Silva, N., Day, T.A., Deplazes, P., Estrada, K., Fernández, C., Holland, P.W.H., Hou, J., Hu, S., Huckvale, T., Hung, S.S., Kamenetzky, L., Keane, J.A., Kiss, F., Koziol, U., Lambert, O., Liu, K., Luo, X., Luo, Y., Macchiaroli, N., Nichol, S., Paps, J., Parkinson, J., Pouchkina-Stantcheva, N., Riddiford, N., Rosenzvit, M., Salinas, G., Wasmuth, J.D., Zamanian, M., Zheng, Y., Garciarrubio, A., Bobes, R.J., Fragoso, G., Sánchez-Flores, A., Estrada, K., Cevallos, M.A., Morett, E., González, V., Portillo, T., Ochoa-Leyva, A., José, M. V., Sciutto, E., Landa, A., Jiménez, L., Valdés, V., Carrero, J.C., Larralde, C., Morales-Montor, J., Limón-Lason, J., Soberón, X., Laclette, J.P., Cai, X., Soberón, X., Olson, P.D., Laclette, J.P., Brehm, K., Berriman, M., 2013. The genomes of four tapeworm species reveal adaptations to parasitism. Nature 496, 57–63. https://doi.org/10.1038/nature12031

Vaca, H.R., Celentano, A.M., Macchiaroli, N., Kamenetzky, L., Camicia, F., Rosenzvit, M.C., 2019. Histone deacetylase enzymes as potential drug targets of Neglected Tropical Diseases caused by cestodes. Int. J. Parasitol. Drugs drug Resist. 9, 120–132. https://doi.org/10.1016/j.ijpddr.2019.02.003

Vaca, H.R., Celentano, A.M., Toscanini, M.A., Heimburg, T., Ghazy, E., Zeyen, P., Hauser, A.-T., Oliveira, G., Elissondo, M.C., Jung, M., Sippl, W., Camicia, F., Rosenzvit, M.C., 2021. The potential for histone deacetylase (HDAC) inhibitors as cestocidal drugs. PLoS Negl. Trop. Dis. 15, e0009226. https://doi.org/10.1371/journal.pntd.0009226

World Health Organization, 2020. Ending the neglect to attain the sustainable development goals: a road map for neglected tropical diseases 2021–2030: overview. World Health Organization, Geneva.

Zhang, Y., Skolnick, J., 2005. TM-align: A protein structure alignment algorithm based on the TM-score. Nucleic Acids Res. 33, 2302–2309. https://doi.org/10.1093/nar/gki524

Zheng, H., Zhang, W., Zhang, L., Zhang, Z., Li, J., Lu, G., Zhu, Y., Wang, Y., Huang, Y., Liu, J., Kang, H., Chen, J., Wang, L., Chen, A., Yu, S., Gao, Z., Jin, L., Gu, W., Wang, Z., Zhao, L., Shi, B., Wen, H., Lin, R., Jones, M.K., Brejova, B., Vinar, T., Zhao, G., McManus, D.P., Chen, Z., Zhou, Y., Wang, S., 2013. The genome of the hydatid tapeworm *Echinococcus granulosus*. Nat. Genet. 45, 1168–1175. https://doi.org/10.1038/ng.2757

Legends to figures

Fig. 1. Chemical structures of the sirtuin inhibitors used in this work: AGK2, EX-527 (Selisistat), Mz236 (SirReal1), and Mz25 (SirReal2).

Fig. 2. Phylogenetic analysis of cestode sirtuin (SIRT) catalytic domains. The figure shows the phylogenetic tree generated by Neighbour-joining analysis (see section 2) to emphasize the relationships between cestode SIRT genes and their orthologs in *Homo sapiens* (*Hs*), *Mus musculus* (*Mm*), *Drosophila melanogaster* (*Dm*), and *Schistosoma mansoni* (*Sm*). SIRT Class I genes are marked in blue, Class II in green, Class III in orange and Class IV in pink. SIRT sequences used were: for cestodes as in Table 1, for *H. sapiens Hs*SIRT1 (Q96EB6), *Hs*SIRT2 (Q8IXJ6), *Hs*SIRT3 (Q9NTG7), *Hs*SIRT4 (Q9Y6E7), *Hs*SIRT5 (Q9NXA8), *Hs*SIRT6 (Q8N6T7), and *Hs*SIRT7 (Q9NRC8); for *M. musculus Mm*SIRT1 (Q923E4), *Mm*SIRT2 (Q8VDQ8), *Mm*SIRT3 (Q8R104), *Mm*SIRT4 (Q8R216), *Mm*SIRT5 (Q8K2C6), *Mm*SIRT6 (P59941), and *Mm*SIRT7 (Q8BKJ9); for *D. melanogaster Dm*SIRT1 (Q9VK34), *Dm*SIRT2 (Q9I7I7), *Dm*SIRT4 (Q8IRR5), and *Dm*SIRT7 (Q9VAQ1); and for *S. mansoni Sm*SIRT1 (ABG78545.1), *Sm*SIRT2 (AGT95745.1), *Sm*SIRT5 (AGT95748.1), *Sm*SIRT6 (AGT95751.1), and *Sm*SIRT7 (AGT95752.1).

Fig. 3. Comparison of sirtuin (SIRT) catalytic domains. Percentage of identity of SIRT catalytic domains between *Homo sapiens* (*Hs*) and the cestodes: *Echinococcus canadensis* (*Ec*), *Echinococcus granulosus sensu stricto* G1 (*Eg*), *Echinococcus multilocularis* (*Em*), *Mesocestoides vogae* (*Mv*), and *Taenia solium* (*Ts*). Each panel shows the percentage of identity for each SIRT gene. The values were taken from a percent identity matrix created by Clustal2.1.

Fig. 4. Transcriptional expression levels of sirtuin (SIRT) genes in *Echinococcus* spp. Comparative transcriptional expression levels of SIRT genes, expressed as Reads Per Kilobase Million mapped reads (RPKM), in several developmental stages of (A) *Echinococcus granulosus sensu strict* G1 (*Eg*): adult, oncospheres (Onc), protoscoleces (PSC), and germinal and laminated layers – or cyst wall – (CW) and (B) *Echinococcus multilocularis* (*Em*): Onc, activated Onc (Act Onc), 4 week metacestodes miniature vesicles (4wCW), and metacestodes small vesicles cultivated in vitro (Cmet).

Fig. 5. Effect of sirtuin (SIRT) inhibitors in *Mesocestoides vogae* tetrathyridia (TTy). (A- D) In vitro cestocidal activity determined for the SIRT inhibitors: (A) AGK2, (B) EX-527, (C) Mz236, and (D) Mz25. The SIRT inhibitors were evaluated at concentrations of 2, 20 and 50 µM and at different incubation times, using the *M. vogae* TTy motility assay. Parasites incubated with the drug vehicle (DMSO 1%) were used as a negative control. Relative motility indices were measured from three independent biological replicates, each one in quadruplicate. Error bars represent the standard deviation and the asterisks indicate those values that showed differences with statistical significance compared with the negative control, according to two-way ANOVA test and Dunnett's post-tests (*$P < 0.05$; **$P < 0.01$; ***$P < 0.001$; ****$P < 0.0001$). (E) Inverted optical microscope images of *M. vogae* TTy treated with Mz25 at 2, 20 and 50 µM at different days of treatment; compared with the parasites incubated with DMSO 1%. Note the extensive damage on the tegument with the presence of blebs (arrows) and needle-like structures (circle); as well as the loss of general parasite morphology with the presence of influx (I) of culture medium into the worm and tegument debris (D) in the culture medium. These phenotypic alterations were observed for three independent biological replicates and were marked in the images at 9 days of treatment. Scale bars represent 100 µm.

Fig. 6. Irreversible effect of the sirtuin inhibitor Mz25 in *Mesocestoides vogae* tetrathyridia (TTy). In vitro cestocidal activity determined for Mz25 and albendazole (ABZ) at different incubation times. The compounds were tested at their respective 90% inhibitory concentration (IC_{90}) concentrations for 6 days, then culture medium was removed, and TTy were gently washed and incubated with a fresh culture medium without adding the compounds for 8 additional days. Parasites incubated with the drug vehicles (DMSO 1%) or parasites pre-treated with 70% ethanol (EtOH 70%) for 30 min were used as controls. Relative motility indices were measured using the *M. vogae* TTy motility assay from three independent biological replicates, each one in quadruplicate. Error bars represent the standard deviation.

Fig. 7. Effect of the sirtuin inhibitor Mz25 on *Mesocestoides vogae* tetrathyridia (TTy) morphology. Scanning electron microscopy images of *M. vogae* treated with (A-C) the drug vehicle 1% DMSO or (D-F) Mz25 at 20 μM after 6 days of incubation and at different magnifications (indicated in each figure). Extensive damage was observed on parasites treated with Mz25, with marked alterations in the tegument and loss of parasite morphology, as well as vesicle-like structures of different sizes in the tegument and a complete loss of microtriches. The sizes of the scale bars are shown in each image.

Fig. 8. Cestode sirtuin 2 (SIRT2) structures by homology modeling. (A) Sequence alignment of SIRT-catalytic domain of SIRT2 proteins from *Homo sapiens* (*Hs*SIRT2), *Schistosoma mansoni* (*Sm*SIRT2) and the cestodes: *Echinococcus canadensis* G7 (*Ec*SIRT2), *Echinococcus granulosus sensu stricto* G1 (*Eg*SIRT2), *Echinococcus multilocularis* (*Em*SIRT2), *Mesocestoides vogae* (*Mv*SIRT2), and *Taenia solium* (*Ts*SIRT2). Sequence identities (≥ 75%) or similarities (≥ 75%) are depicted in light and dark green, respectively. Conserved residues involved in zinc coordination (rhombus) or NAD^+ binding

(arrow) are indicated below the alignment. (B) Superposition of *Hs*SIRT2 (PDB ID: 4RMG; blue) and the homology models obtained for *Ec*SIRT2 (red), *Eg*SIRT2 (orange), *Em*SIRT2 (purple), *Mv*SIRT2 (pink), and *Ts*SIRT2 (cyan). All SIRT2 enzymes share a similar domain architecture. The yellow sphere represents the ion zinc (Zn^{2+}); while NAD^+ molecule (green) is shown as sticks. (C) Ribbon representation of the active site of SIRT2 enzymes. Interaction of Mz25 with SIRT2 enzymes from human or cestodes in complex with the cofactor NAD^+. Mz25 (yellow), NAD^+ (green), and interacting residues (conserved residues in white and mutated residues in the corresponding color for each SIRT2 enzyme) are represented as sticks. (For interpretation of the references to colour in this figure legend, the reader is referred to the on-line version of this article.)

Supplementary legends

Supplementary Table S1. Cestode genomes used in this work.

Supplementary Table S2. Numerical data obtained in this work. Excel spreadsheet containing, in separate sheets, the underlying numerical data for Figs. 5A, 5B, 5C, 5D, 6, and Table 2 in the main text.

Supplementary Table S3. Parameters determined for the structure homology models performed to SIRT2 from the cestodes: *Echinococcus canadensis* G7 (*Ec*SIRT2), *Echinococcus granulosus sensu stricto* G1 (*Eg*SIRT2), *Echinococcus multilocularis* (*Em*SIRT2), *Mesocestoides vogae* (*Mv*SIRT2), and *Taenia solium* (*Ts*SIRT2) compared to SIRT2 from *Homo sapiens* (*Hs*SIRT2).

Supplementary Data S1. Supplementary information of SIRT gene annotation in cestode genomes.

Supplementary Fig. S1. Residues implicated in zinc coordination for sirtuin 2 (SIRT2) from *Homo sapiens* (*Hs*SIRT2) and cestodes: *Echinococcus canadensis* G7 (*Ec*SIRT2), *Echinococcus granulosus sensu stricto* G1 (*Eg*SIRT2), *Echinococcus multilocularis* (*Em*SIRT2), *Mesocestoides vogae* (*Mv*SIRT2), and *Taenia solium* (*Ts*SIRT2).

Supplementary Fig. S2. Ramachandran plots determined for the homology structure model of sirtuin 2 gene from *Echinococcus canadensis* G7 (*Ec*SIRT2).

Supplementary Fig. S3. Ramachandran plots determined for the homology structure model of sirtuin 2 gene from *Echinococcus granulosus sensu stricto* G1 (*Eg*SIRT2).

Supplementary Fig. S4. Ramachandran plots determined for the homology structure model of sirtuin 2 gene from *Echinococcus multilocularis* (*Em*SIRT2).

Supplementary Fig. S5. Ramachandran plots determined for the homology structure model of sirtuin 2 gene from *Mesocestoides vogae* (*Mv*SIRT2).

Supplementary Fig. S6. Ramachandran plots determined for the homology structure model of sirtuin 2 gene from *Taenia solium* (*Ts*SIRT2).

Table 1. Sirtuin (SIRT) -encoding genes identified in parasites of the class Cestoda.

Tapeworm species	SIRT-encoding genes (Gene IDs[a])	Size (aa)	CDS localization (scaffold: CDS start-end and strand)	Closest ortholog in *Homo sapiens*		
				Sirtuin	E-value	Identity (%)
Echinococcus canadensis G7	***Ec*SIRT1** (EcG7_01898)	740	E.canG7_contigs_5961: 44824-49438 forward strand	SIRT1	3.00E-119	42
	***Ec*SIRT2** (EcG7_03059)	333	E.canG7_contigs_1852: 67942-70781 reverse strand	SIRT2	1.00E-98	48
	***Ec*SIRT3** (EcG7_05989)	433	E.canG7_contigs_6259: 53750-57293 reverse strand	SIRT3	1.00E-99	54
	***Ec*SIRT6** (EcG7_02911)	391	E.canG7_contigs_7247: 101495-106138 forward strand	SIRT6	8.00E-96	47
	***Ec*SIRT7** (EcG7_08393)	201	E.canG7_contigs_5935: 13154-13905 forward strand	SIRT7	2.00E-37	49
Echinococcus granulosus sensu stricto G1	*Eg*SIRT1 (EgrG_000698900/EGR_03567)	740	pathogen_EgG_scaffold_0013: 1612894-1617506 forward strand	SIRT1	4.00E-121	43
	***Eg*SIRT2** (EgrG_001065100/EGR_05039)	333	EG_S00035: 33730-36500 forward strand	SIRT2	5.00E-98	48
	*Eg*SIRT3 (EgrG_001176600/EGR_03429)	433	pathogen_EgG_scaffold_0012: 1433448-1436989 reverse strand	SIRT3	9.00E-99	53
	*Eg*SIRT5 (EGR_00605)	305	EG_S00002: 2402558-2406585 forward strand	SIRT5	8.00E-97	56
	*Eg*SIRT6 (EgrG_000908100/EGR_00437)	391	EG_S00002: 397358-401997 reverse strand	SIRT6	5.00E-96	47
	***Eg*SIRT7** (EgrG_000740200/EGR_08353)	368	pathogen_EgG_scaffold_0001: 255819-259837 forward strand	SIRT7	6.00E-45	33
Echinococcus multilocularis	*Em*SIRT1 (EmuJ_000698900)	740	pathogen_EmW_scaffold_03: 9696919-9701528 reverse strand	SIRT1	8.00E-120	42
	*Em*SIRT2 (EmuJ_001065100)	333	pathogen_EmW_scaffold_02: 13284798-13287647 forward strand	SIRT2	4.00E-98	47
	*Em*SIRT3 (EmuJ_001176600)	433	pathogen_EmW_scaffold_01: 18349083-18352443 reverse strand	SIRT3	2.00E-98	53
	***Em*SIRT6** (EmuJ_000908100)	382	pathogen_EmW_scaffold_01: 15319006-15323535 forward strand	SIRT6	2.00E-96	47
	***Em*SIRT7** (EmuJ_000740200)	360	pathogen_EmW_scaffold_01: 195889-199741 forward strand	SIRT7	6.00E-46	34
Mesocestoides vogae	*Mv*SIRT1 (MCU_006369-RB)	302	MCOS_contig0000192: 56-2096 reverse strand	SIRT1	4.00E-85	60
	*Mv*SIRT2 (MCU_003326-RC)	334	MCOS_scaffold0000155: 95906-101061 reverse strand	SIRT2	3.00E-96	46

	*Mv*SIRT3 (MCU_001891-RA)	424	MCOS_scaffold0000077: 53562-56847 reverse strand	SIRT3	6.00E-97	52
	*Mv*SIRT5 (MCU_008975-RB)	270	MCOS_scaffold0000560: 27940-33685 reverse strand	SIRT5	2.00E-108	58
	***Mv*SIRT6** (MCU_009318)	413	MCOS_scaffold0000599: 12561-16176 reverse strand	SIRT6	1.00E-84	43
	***Mv*SIRT7 (**MCU_013737)	210	MCOS_contig0002186: 1204-2458 forward strand	SIRT7	5.00E-39	54
Taenia solium	***Ts*SIRT1** (TsM_000843700)	736	pathogen_TSM_contig_00202: 77962-82932 forward strand	SIRT1	7.00E-118	42
	*Ts*SIRT2 (TsM_000579800)	333	pathogen_TSM_contig_00039: 234248-236912 reverse strand	SIRT2	3.00E-99	49
	***Ts*SIRT3** (TsM_000282000)	432	pathogen_TSM_contig_00455: 10766-13817 forward strand	SIRT3	1.00E-97	53
	***Ts*SIRT6** (TsM_000857100)	391	pathogen_TSM_contig_00237: 86350-90937 forward strand	SIRT6	1.00E-97	48
	***Ts*SIRT7** (TsM_000486400)	366	pathogen_TSM_contig_01179: 14489-18318 forward strand	SIRT7	3.00E-45	35

[a]Gene IDs acording to the genome annotation in the WormBase Parasite database. SIRT-encoding genes in bold were re-annotated in this work (see Supplementaty Data S1 for a detail of SIRT-encoding genes annotation). The information and values reported for these genes in this table were obtained used these re-annotated SIRT-encoding genes.

aa, amino acids.

Table 2. In vitro cestocidal activity of the selective sirtuin 2 (SIRT2) inhibitor Mz25 and the current anthelmintic drug albendazole in *Mesocestoides vogae* tetrathyridia.

Compounds	Dose–response relationship parameters[a]		
	IC_{25} ± S.D. (µM)	IC_{50} ± S.D. (µM)	IC_{90} ± S.D. (µM)
Mz25	15.11 ± 3.20	17.20 ± 2.62	23.11 ± 0.70
ABZ	15.82 ± 0.56	20.59 ± 0.38	36.01 ± 2.00

[a]The half-maximal (IC_{50}), 90% (IC_{90}), and 25% (IC_{25}) inhibitory concentration values were calculated from three independent biological replicates, each one in quadruplicate, and were expressed with their respective S.D.

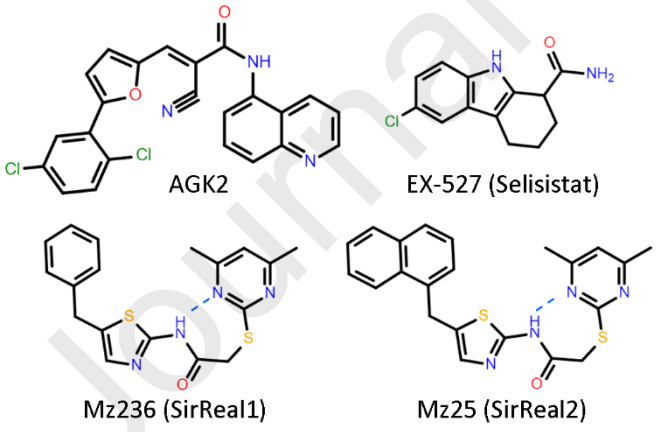

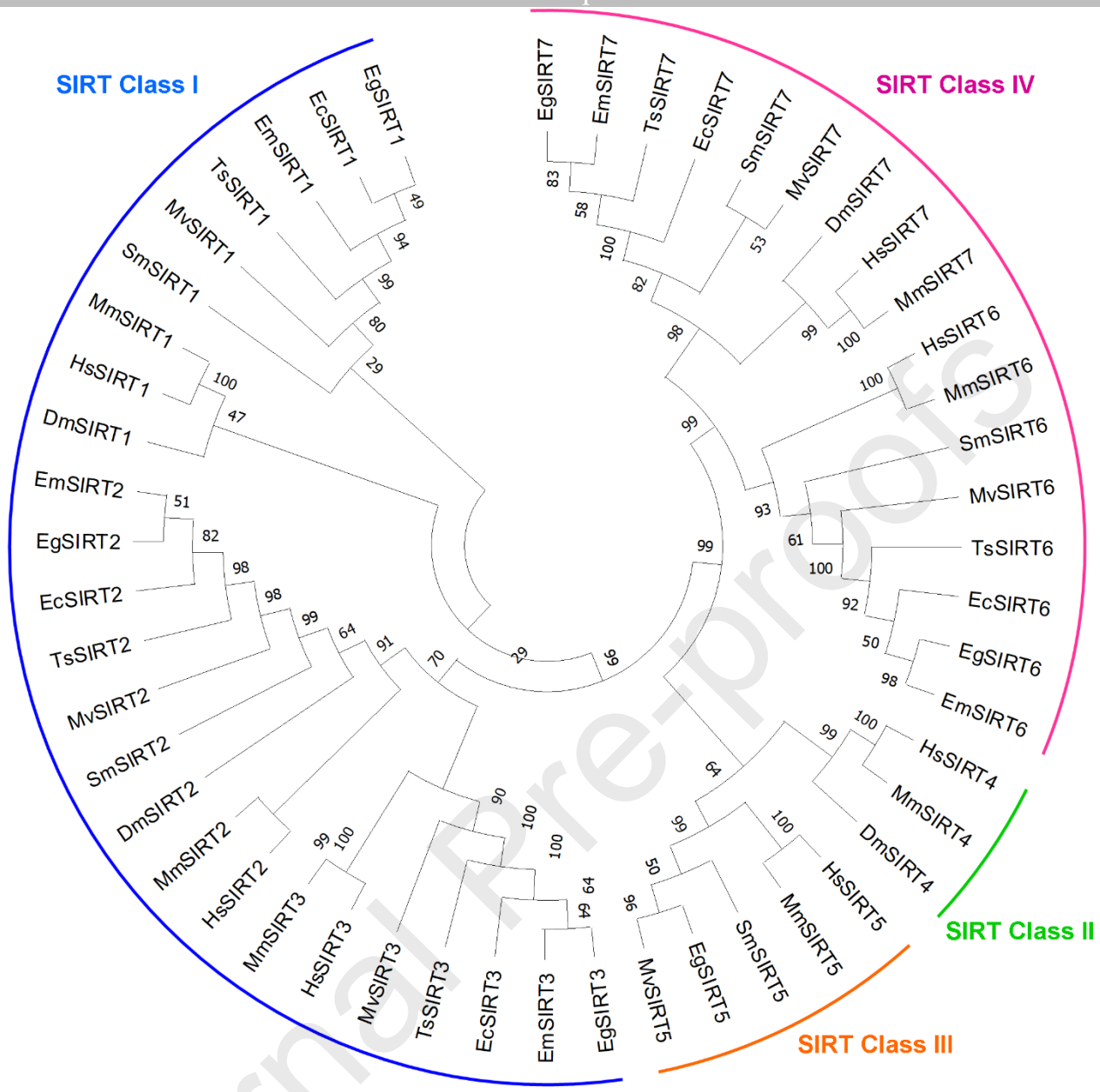

	Hs SIRT1
Ec SIRT1	65.78%
Eg SIRT1	65.78%
Em SIRT1	65.24%
Mv SIRT1	72.46%
Ts SIRT1	66.31%

	Hs SIRT2
Ec SIRT2	62.30%
Eg SIRT2	62.30%
Em SIRT2	61.75%
Mv SIRT2	59.56%
Ts SIRT2	61.75%

	Hs SIRT3
Ec SIRT3	60.99%
Eg SIRT3	60.99%
Em SIRT3	60.99%
Mv SIRT3	60.44%
Ts SIRT3	61.54%

	Hs SIRT5
Eg SIRT5	57.87%
Mv SIRT5	62.76%

	Hs SIRT6
Ec SIRT6	56.80%
Eg SIRT6	56.80%
Em SIRT6	57.40%
Mv SIRT6	55.03%
Ts SIRT6	57.40%

	Hs SIRT7
Ec SIRT7	53.06%
Eg SIRT7	46.84%
Em SIRT7	46.84%
Mv SIRT7	56.25%
Ts SIRT7	46.84%

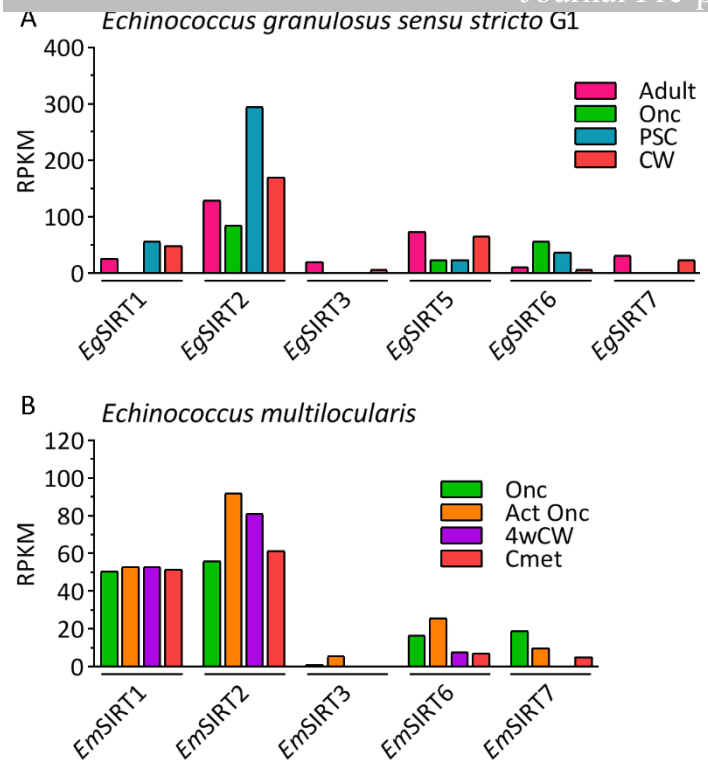

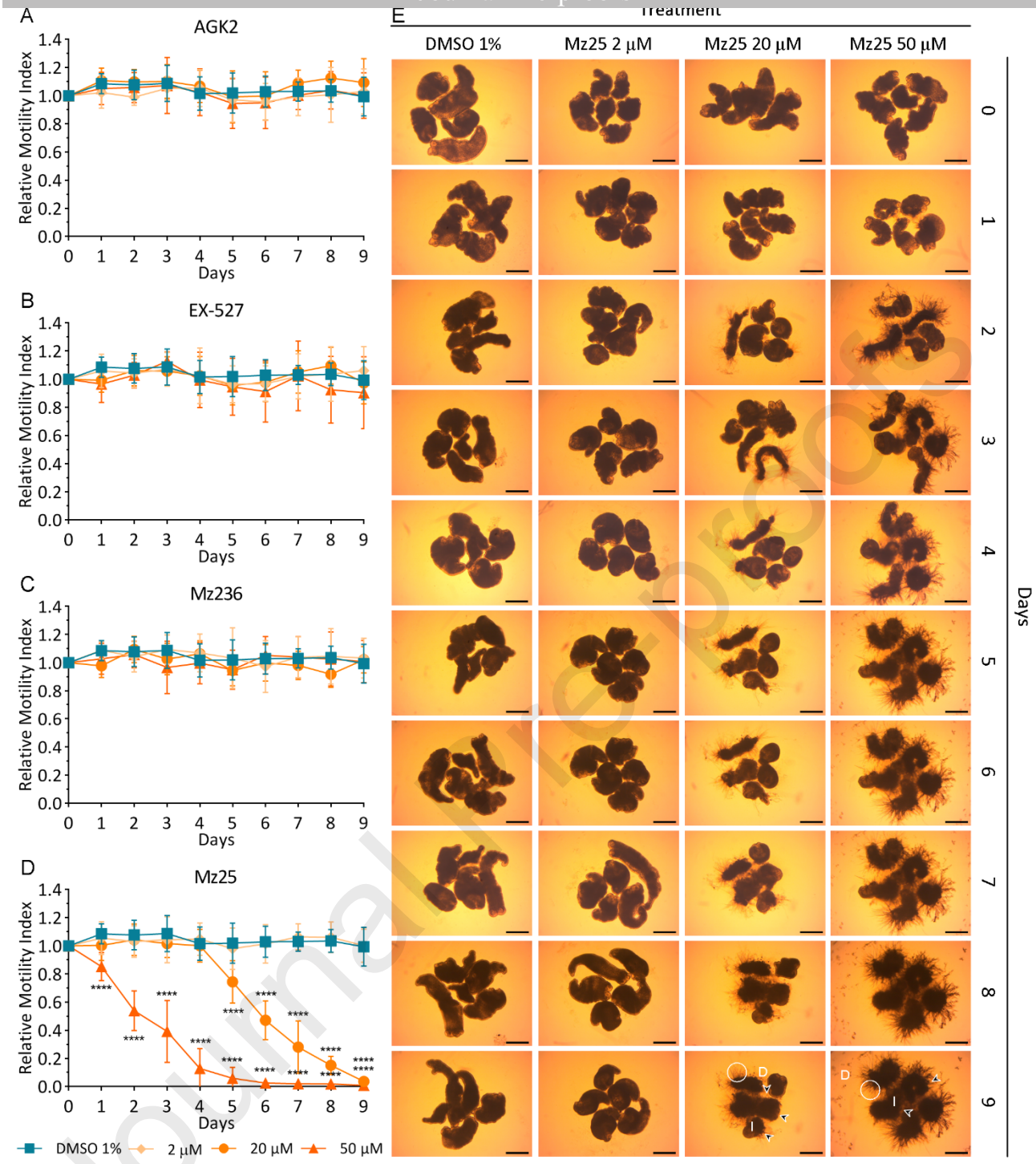

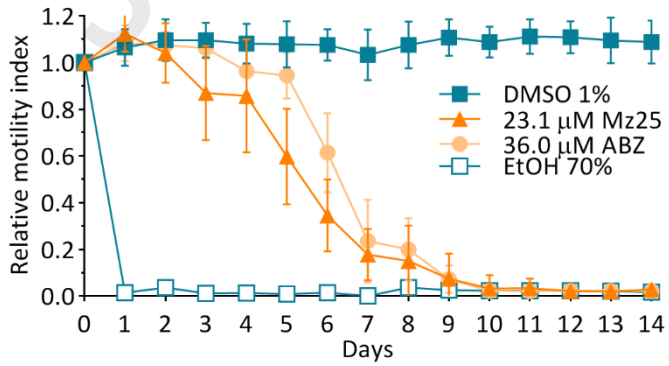

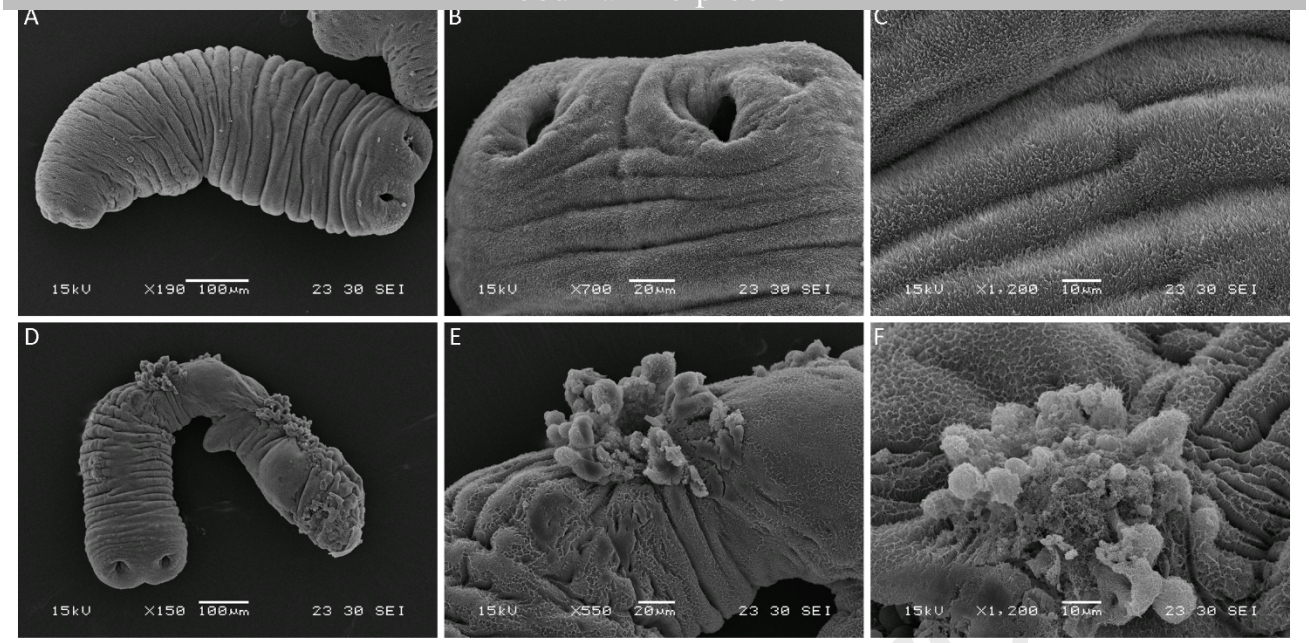

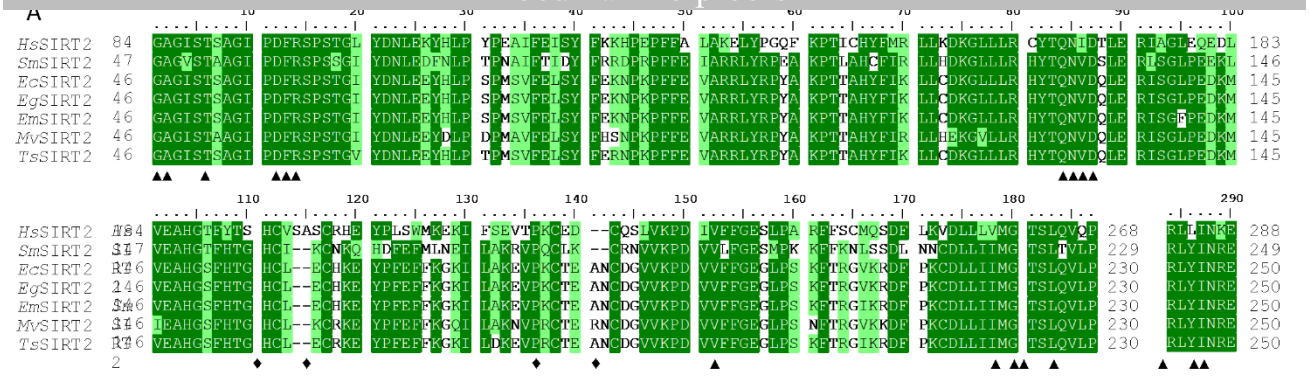
A
HsSIRT2
SmSIRT2
EcSIRT2
EgSIRT2
EmSIRT2
MvSIRT2
TsSIRT2

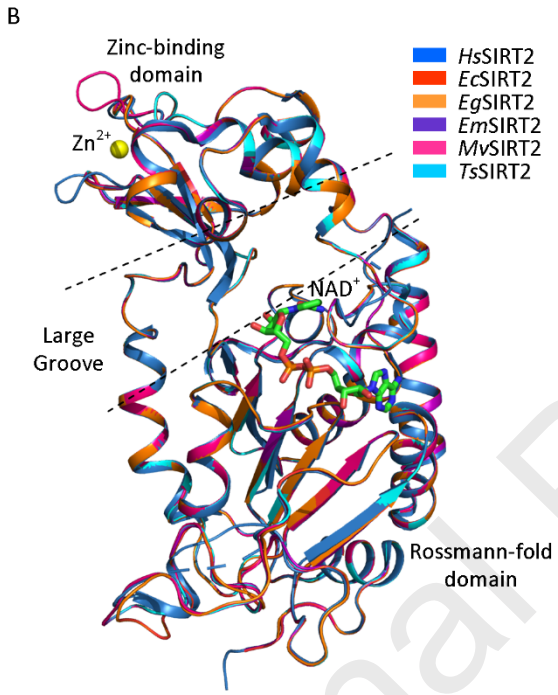
B
Zinc-binding domain
Zn2+
NAD+
Large Groove
Rossmann-fold domain
HsSIRT2
EcSIRT2
EgSIRT2
EmSIRT2
MvSIRT2
TsSIRT2

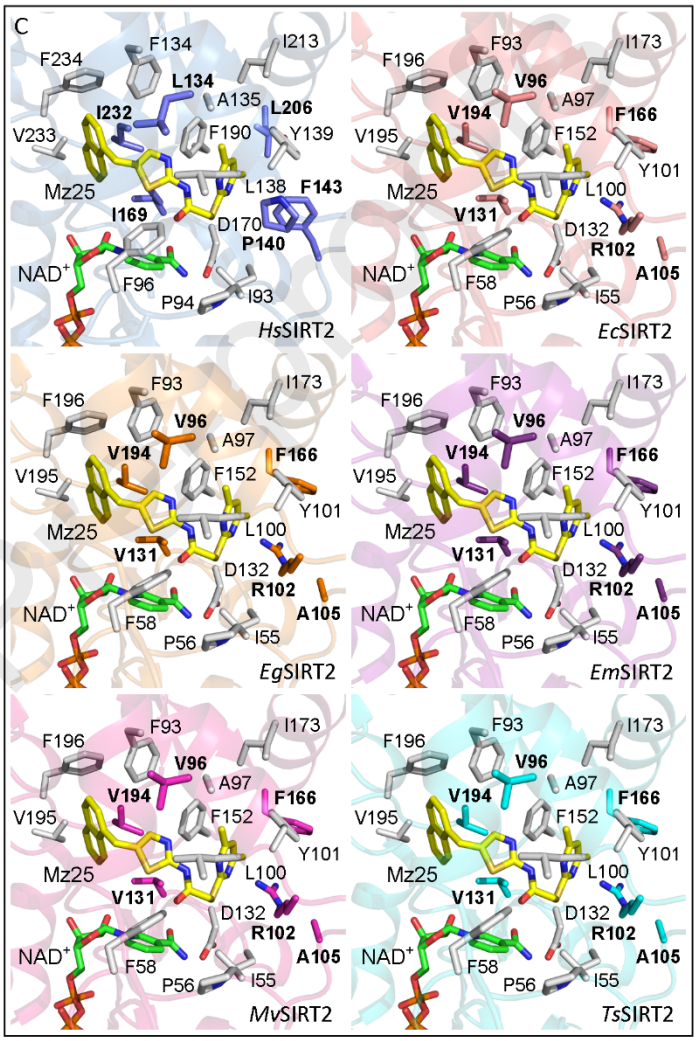
C
HsSIRT2
EcSIRT2
EgSIRT2
EmSIRT2
MvSIRT2
TsSIRT2
NAD+

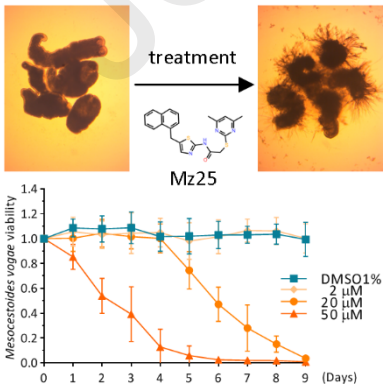
treatment
Mz25
Mesocestoides vogae viability
DMSO1%
2 µM
20 µM
50 µM
(Days)

HIGHLIGHTS

Cestode genomes contain six SIRT-encoding genes classified into classes I, III and IV

Class I SIRTs are the most expressed in several developmental stages of *Echinococcus*

SIRT2 inhibitor Mz25 has a strong cestocidal activity in *Mesocestoides vogae* larvae

Mz25 cestocidal activity is irreversible and time- and dose-dependent